

# Characterization of Platinum on Sulfated Zirconia Catalysts by Temperature Programmed Reduction

Awa Dicko, Xuemin Song, Alain Adnot, and Abdelhamid Sayari<sup>1</sup>

Department of Chemical Engineering and CERPIC  
Université Laval, Ste-Foy, Québec, Canada G1K 7P4

Received March 7, 1994; revised June 17, 1994

Temperature programmed reduction, X-ray photoelectron spectroscopy, and X-ray diffraction were used for comparative characterization of Pt on sulfated and nonsulfated zirconia catalysts calcined both *in situ* and *ex situ* at different temperatures in the range 25–800°C. The effect of sulfur species on the state of Pt was twofold. They decreased the interactions between Pt oxide and the support, thus leading to large particles easy to decompose into large metallic Pt particles that resisted reoxidation in air. In the absence of sulfur species, up to a calcination temperature of 650°C, Pt oxide and metallic Pt particles remained small. Such samples underwent almost complete reoxidation during storage in air. Sulfur species also had a direct effect on the state of Pt. Sulfur dioxide produced by decomposition of sulfate played the role of a reducing agent. Under temperature programmed reduction conditions, two sulfate reduction peaks were obtained regardless of the presence of Pt. The occurrence of two different sulfate species was suggested and a tentative assignment proposed. © 1994 Academic Press, Inc.

## INTRODUCTION

Sulfated zirconia superacid catalysts have been the subject of several recent reviews (1–4). Addition of small amounts of transition metals was found to greatly improve the hydroisomerization activity of these catalysts as well as their stability (5, 6). Platinum was found to be the most effective metal (4). Most of the characterization studies reported so far deal with the acid support rather than the metallic component of the catalyst (1, 2). Calcination of these catalysts typically at 600–650°C is a crucial requisite for catalytic activity. However, even when previously calcined, these catalysts have to undergo a heat treatment under air or inert gas immediately before use to exhibit any significant catalytic activity (7).

Usually Pt on sulfated zirconia catalysts are not hydrogen reduced before use. However, since typical applica-

tions take place under hydrogen at 150–250°C (1, 2), it was until recently implicitly understood that the noble metal is reduced under reaction conditions. It is true that platinum on sulfated zirconia does not readily exhibit metallic properties even after H<sub>2</sub> reduction. For example such samples have very low hydrogenation activity (8) and hardly chemisorb CO or H<sub>2</sub> at room temperature (7, 9). Such behavior may simply be attributable to sulfur poisoning of metallic platinum (8, 10, 11). However, based on X-ray photoelectron spectroscopy (XPS) data, Ebitani *et al.* (9) reported that Pt on sulfated zirconia remains essentially in an oxidized state, even after hydrogen treatment at 400°C. They found that only about 15% of Pt was in the metallic state. These findings led the authors to conclude that the lack of chemisorption and hydrogenation ability is due to the oxidation state of platinum rather than to sulfur poisoning of metallic platinum (9). Nonetheless, such a conclusion is intriguing, first because supported platinum catalysts are usually easy to reduce (12, 13), and second because at higher temperatures (100–300°C) Pt on sulfated zirconia catalysts adsorb large amounts of hydrogen (14). Moreover, based on the XPS analysis of a EUROPT-1 catalyst pretreated under different conditions (oxidation, reduction, and sulfidation), Paál *et al.* (15) questioned the conclusions put forward by Ebitani *et al.* (9).

In a previous paper (16) we used XPS, X-ray diffraction, and temperature programmed reduction (TPR) to demonstrate that Pt on sulfated zirconia actually reduces to the metallic state upon air calcination at 600°C. We also proposed that the Pt was reduced by SO<sub>2</sub> which was released during calcination. However, all samples were studied after calcination in static air and storage under ambient conditions. Therefore, the state of platinum was due to a combined effect of the calcination conditions and possibly reoxidation during storage. The main objective of this paper was to shed further light on the state of Pt on sulfated zirconia after calcination at various temperatures and to distinguish between the actual effect of calcination and the effect of further reoxidation of reduced platinum

<sup>1</sup> To whom correspondence should be addressed. Fax: 418-656 5993. E-mail: sayari@gch.ulaval.ca.

during storage. For comparison, two series of samples, one with no platinum and the other with no sulfate, were also studied. The main technique used was TPR.

### EXPERIMENTAL

Zirconium hydroxide was prepared by hydrolysis of zirconyl chloride (98%, Aldrich) with aqueous ammonium hydroxide (28 wt%, Anachemia) at room temperature. The solid was then filtered and thoroughly washed in order to free it of chloride ions, and dried in air at 50°C for several days. Sulfation of zirconium hydroxide was carried out by mixing it with a 1 N sulfuric acid solution. The amount of acid solution was 10 ml per gram of zirconium hydroxide. After 1 h of stirring, the solid was filtered and dried again at 110°C before storage.

Platinum was loaded on both sulfated and nonsulfated zirconia as  $\text{H}_2\text{PtCl}_6$  using the incipient wetness method. Typically platinum content should be kept below 1 wt%; however, in this study a high metal loading (4–5 wt%) was used to make characterization easier. Sulfated and nonsulfated samples were calcined in air for 2 h at different temperatures up to 800°C. Depending on whether it was sulfated or not, a sample will be referred to as  $\text{Pt}/\text{ZrO}_2/\text{SO}_4^-/t_c$  or  $\text{Pt}/\text{ZrO}_2/t_c$ , respectively. In this nomenclature,  $t_c$  stands for the calcination temperature in °C. Samples that do not contain platinum will be designated as  $\text{ZrO}_2/\text{SO}_4^-/t_c$  or  $\text{ZrO}_2/t_c$  depending on whether they were sulfated or not. On occasions,  $\text{PtCl}_4$  was used instead of  $\text{H}_2\text{PtCl}_6$  and also zirconium sulfate  $\text{ZrOSO}_4$  was used as a support. The actual Pt loading was measured by atomic absorption using a Varian 300 spectrometer.

Temperature programmed experiments were carried out using an automated Altamira AM11 instrument. In a typical TPR experiment, about 100 to 120 mg of precalcined sample was loaded in a quartz microreactor which was then installed in a furnace coupled to a temperature controller/programmer. A thermocouple was placed in the catalyst bed to monitor its temperature. The catalyst was first exposed to flowing argon and the temperature was raised at a rate of 10°C/min up to  $t_c$  or 300°C, whichever is lower, and was kept at that temperature for 0.5 h before cooling to room temperature. Subsequently the sample was heated under a flowing gas mixture of 10%  $\text{H}_2$  in argon up to 750°C. The heating rate was 10°C/min. Another series of TPR experiments were conducted using a different *in situ* pretreatment in flowing air instead of flowing argon. The samples used for these experiments were predried at 100°C, but not precalcined. Once loaded in a quartz microreactor, the samples were heated under flowing dry air at different temperatures for 2 h, then cooled under argon before undergoing TPR as described above. By comparing the results of both procedures, it will be possible to discriminate between the real effect

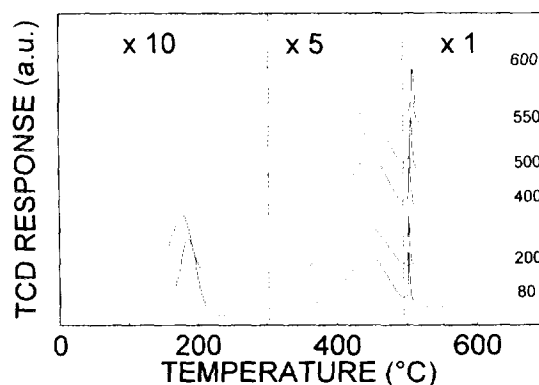


FIG. 1. TPR profile of  $\text{Pt}/\text{ZrO}_2/\text{SO}_4^-/t_c$ . The numbers on the right-hand side indicate the values of  $t_c$  in °C. The numbers at the top represent relative gain.

of calcination and the possible reoxidation of reduced platinum during storage under ambient conditions. In order to check if any reduction took place at ambient temperature, an appropriate number of 0.1  $\text{cm}^3$  pulses of 10%  $\text{H}_2/\text{Ar}$  were used at 30°C.

All gases used were of UHP grade from Liquid Air and Air Products. They were further purified by passage through oxygen and water traps. Analysis of the reactor outlet gas was performed by TCD and by mass spectrometry (MS). A transpector quadrupole from Leybold Inficon, Inc. was used.

XPS spectra were recorded using a V. G. Scientific Escalab Mark II system with a hemispherical electron energy analyzer operated in the constant pass energy mode (20 eV). A  $\text{MgK}\alpha$  X-ray source ( $h\nu = 1253.6$  eV) was used. A reactor was directly connected to the XPS instrument, thus allowing for *in situ* treatment and XPS analysis without air exposure. A binding energy of 182.7 eV for  $\text{Zr}(3d_{5/2})$  level was used as an internal reference for all samples. The binding energy of  $\text{Zr}(3d_{5/2})$  was determined with reference to  $\text{Au}(4f_{7/2}) = 84.0$  eV in duplicate experiments using gold sputtered samples because of interference between  $\text{Pt}(4f)$  and  $\text{Au}(4f)$  peaks.

XRD spectra were recorded on a Philips PW1010 X-ray diffractometer using a nickel-filtered  $\text{CuK}\alpha$  ( $\lambda = 1.506$  Å) radiation.

### RESULTS

Figure 1 shows TPR profiles for a series of  $\text{Pt}/\text{ZrO}_2/\text{SO}_4^-/t_c$  samples precalcined *ex situ* in air at  $t_c$  in the range of 80–600°C. At calcination temperatures below 550°C, TPR spectra exhibit three major features, a peak below 200°C, another at about 450°C, and a sharp peak at 550°C. For  $t_c \geq 600^\circ\text{C}$ , both the low (<200°C) and the high (550°C) temperature peaks disappear. The temperature of the

TABLE 1  
TPR Data of Pt on Sulfated and Nonsulfated Zirconia

$t_c$ (°C) <sup>a</sup>	Pt/ZrO <sub>2</sub> /SO <sub>4</sub> <sup>2-</sup> / $t_c$		Pt/ZrO <sub>2</sub> / $t_c$	
	$T_r$ (°C) <sup>b</sup>	Area <sup>c</sup>	$T_r$ (°C) <sup>b</sup>	Area <sup>c</sup>
80	177	100	175	100
200	169	98	180	106
300	146	102	—	—
400	128	85	176	104
500	104	81	—	—
550	95	58	—	—
600	—	0	122	102
650	—	—	111/186	89
700	—	—	182/258	52
800	—	0	—	0

<sup>a</sup> Calcination temperature.

<sup>b</sup> Temperature of Pt reduction TPR peak.

<sup>c</sup> Normalized area.

peak below 200°C and its relative area are given in Table 1 as functions of calcination temperature. It is seen that as  $t_c$  increases, this peak becomes broader and shifts to lower temperatures. However, the normalized area of the peak did not change significantly for calcination temperatures up to 300°C. This area decreases for samples precalcined between 300 and 600°C.

Analysis of the gas phase by mass spectrometry carried out during the TPR experiment on Pt/ZrO<sub>2</sub>/SO<sub>4</sub><sup>2-</sup>/300 revealed that the appearance of the TPR peak below 200°C was accompanied only by a decrease in the hydrogen partial pressure. Figure 2 shows the variation of the gas phase composition during the appearance of the 450 and 505°C peaks of Fig. 1. It is seen that at the same time as the TPR 450°C peak develops, the fragment of mass 2 amu, i.e., H<sub>2</sub>, decreases while H<sub>2</sub>S fragments (32, 33, and

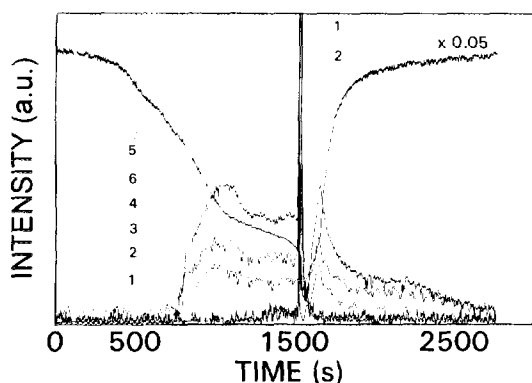


FIG. 2. TPR-MS profile of Pt/ZrO<sub>2</sub>/SO<sub>4</sub><sup>2-</sup>/300; the values of  $m/e$  are (1) 64, (2) 48, (3) 32, (4) 34, (5) 2, and (6) 33. (The origin of the x-axis is arbitrary.)

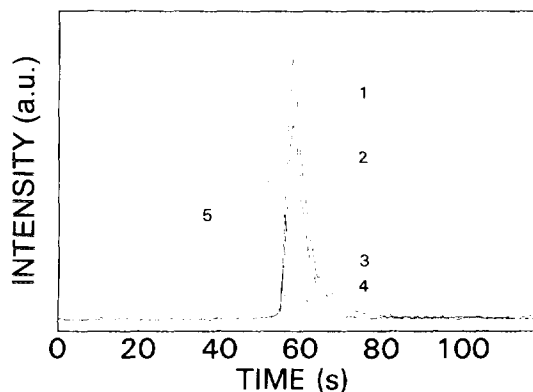


FIG. 3. TPR-MS profile of Pt/ZrO<sub>2</sub>/SO<sub>4</sub><sup>2-</sup>/300. Enlargement of the central part of Fig. 2. The values of  $m/e$  are (1) 64, (2) 48, (3) 32, (4) 34, and (5) 2. (The origin of the x-axis is arbitrary.)

34 amu) increase. This indicates that the 450°C peak is attributable to H<sub>2</sub>S evolution and H<sub>2</sub> consumption. The crowded area at around 1500 s in Fig. 2, which corresponds to the development of the TPR 505°C peak, is enlarged and shown in Fig. 3. It is seen that as the TPR 505°C peak develops, the MS peaks corresponding to SO<sub>2</sub> fragmentation (32, 48, and 64 amu) increase sharply while the H<sub>2</sub> peak decreases further. It is therefore concluded that the TPR 505°C peak corresponds to the simultaneous release of SO<sub>2</sub> and consumption of hydrogen.

Figure 4 shows TPR profiles of a series of ZrO<sub>2</sub>/SO<sub>4</sub><sup>2-</sup>/ $t_c$  samples. Up to a calcination temperature of ca. 500°C, the TPR spectra exhibited two peaks at ca. 640–670°C and 710–725°C. When  $t_c$  exceeds 600°C, only the low temperature peak persisted. Figure 5 illustrates the changes in the concentration of appropriate fragments in the mass spectrometer during the same time the TPR peaks were developing. It is seen that both TPR peaks are due to the consumption of H<sub>2</sub> and the release of SO<sub>2</sub>.

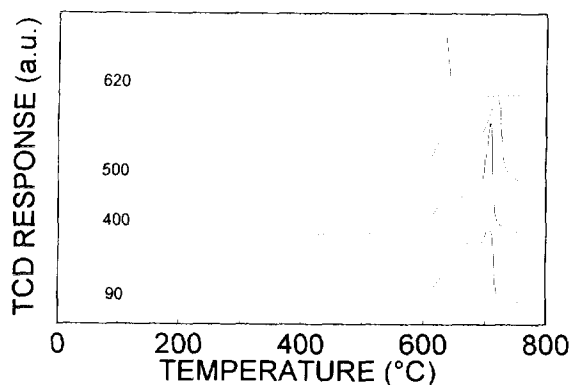


FIG. 4. TPR profile of ZrO<sub>2</sub>/SO<sub>4</sub><sup>2-</sup>/ $t_c$ . The numbers on the left-hand side indicate the values of  $t_c$  in °C.

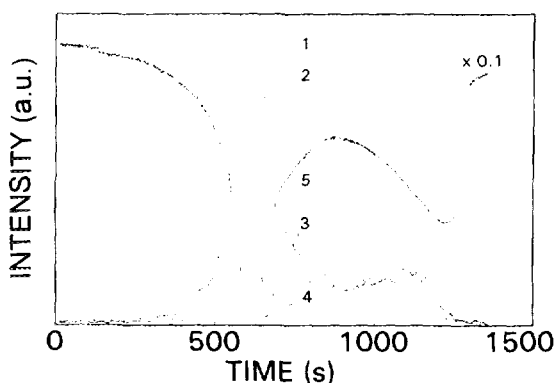


FIG. 5. TPR-MS profile of  $\text{ZrO}_2/\text{SO}_4^{2-}/400$ ; the values of  $m/e$  are (1) 64, (2) 48, (3) 32, (4) 34, and (5) 2. (The origin of the x-axis is arbitrary.)

Note that during TPR of Pt-free sulfated samples no  $\text{H}_2\text{S}$  was detected, whereas for  $\text{Pt}/\text{ZrO}_2/\text{SO}_4^{2-}/t_c$  both  $\text{SO}_2$  and  $\text{H}_2\text{S}$  were observed (Fig. 2).

TPR profiles for nonsulfated  $\text{Pt}/\text{ZrO}_2/t_c$  samples precalcined *ex-situ* at 200–800°C are shown in Fig. 6. TPR peaks maxima along with their normalized areas are summarized in Table 1. For  $t_c \leq 400^\circ\text{C}$ , the platinum reduction peak appears at ca. 175°C. As the calcination temperature increases to ca. 650°C, the TPR peak broadens, but its normalized total area remains constant (Table 1). At  $t_c = 700^\circ\text{C}$ , the TPR peak becomes even broader and its total area decreases. Finally, as shown in Fig. 6, the  $\text{Pt}/\text{ZrO}_2/800$  did not exhibit any TPR feature.

Figure 7 shows the X-ray diffraction patterns of  $\text{ZrO}_2/800$  along with  $\text{Pt}/\text{ZrO}_2/\text{SO}_4^{2-}/600$  and  $\text{Pt}/\text{ZrO}_2/800$ . Both Pt containing samples clearly show the presence of peaks attributable to metallic Pt (Figs. 7b and 7c). In addition, as reported in the literature (1, 2), in sulfate-free samples, both the tetragonal and monoclinic  $\text{ZrO}_2$  phases were

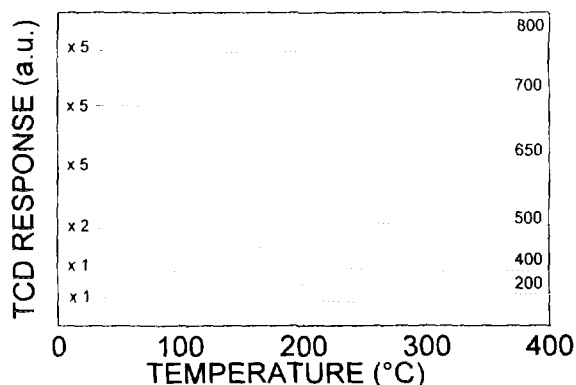


FIG. 6. TPR profile of  $\text{Pt}/\text{ZrO}_2/t_c$ . The numbers on the right-hand side indicate the values of  $t_c$  in  $^\circ\text{C}$ . The numbers on the left-hand side represent relative gain.

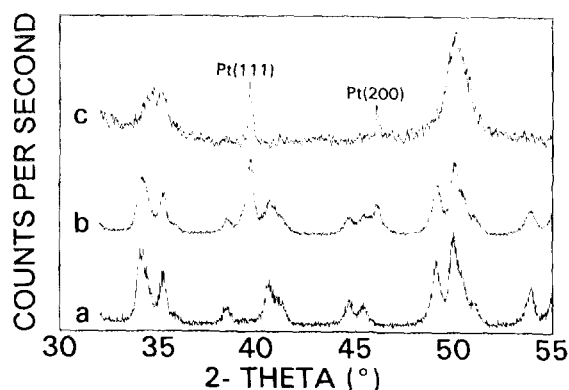


FIG. 7. X-ray diffraction pattern of (a)  $\text{ZrO}_2/800$ , (b)  $\text{Pt}/\text{ZrO}_2/800$ , and (c)  $\text{Pt}/\text{ZrO}_2/\text{SO}_4^{2-}/600$ .

present, whereas the sulfated catalyst showed mostly tetragonal zirconia.

The composition of the gas phase during TPR of a sample containing 4 wt% Pt on zirconium sulfate  $\text{ZrOSO}_4$  precalcined at 300°C was monitored by TCD and by mass spectrometry. During TPR there was no consumption of hydrogen below 300°C. In the temperature range corresponding to the reduction of sulfate species, only one relatively broad peak, the maximum of which was at 538°C, was recorded by TCD. However, as seen in Fig. 8, mass spectrometry analysis shows two distinct features: a small low-temperature peak corresponding to  $\text{H}_2$  consumption (2 amu) and  $\text{H}_2\text{S}$  formation (34 amu), and a strong high-temperature peak corresponding to the consumption of  $\text{H}_2$  (2 amu) and the formation of  $\text{SO}_2$  (64 amu). This indicates the presence of two sulfate species, one of which reduces to  $\text{H}_2\text{S}$  and the other of which reduces at a higher temperature to  $\text{SO}_2$ . Conversely to sulfated samples (Figs. 1 and 2) the TPR of Pt on zirconium sulfate generates much more  $\text{SO}_2$  than  $\text{H}_2\text{S}$ .

TPR experiments of predried samples carried out after *in situ* calcination generated the data shown in Fig. 9B.

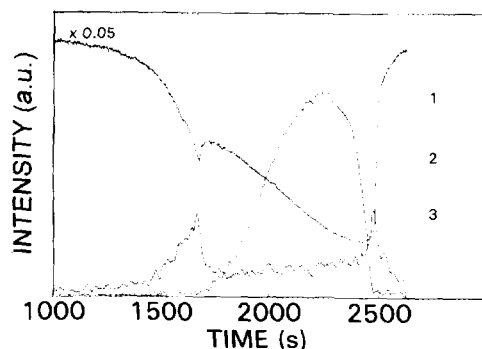


FIG. 8. TPR-MS profile of  $\text{PtCl}_4/\text{ZrOSO}_4/300$ ; the values of  $m/e$  are (1) 2, (2) 64, and (3) 34. (The origin of the x-axis is arbitrary.)

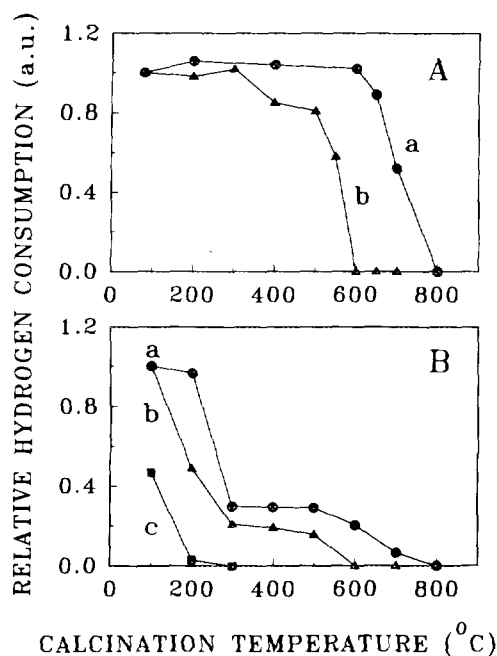


FIG. 9. TPR data: normalized Pt reduction peak area vs calcination temperature; (A) *ex situ* precalcined samples; (B) *in situ* calcined samples; (a) Pt/ZrO<sub>2</sub>; (b) Pt/ZrO<sub>2</sub>/SO<sub>4</sub><sup>2-</sup>; (c) PtCl<sub>4</sub>/ZrOSO<sub>4</sub>.

Three samples predried at 100°C were studied: Pt/ZrO<sub>2</sub>, Pt/ZrO<sub>2</sub>/SO<sub>4</sub><sup>2-</sup>, and Pt/ZrOSO<sub>4</sub>. Fig. 9B shows the area of the Pt reduction peak obtained during TPR vs the *in situ* calcination temperature. All data were normalized taking into account the actual Pt content. For easy comparison, data obtained during TPR of precalcined Pt/ZrO<sub>2</sub>/*t<sub>c</sub>* and Pt/ZrO<sub>2</sub>/SO<sub>4</sub><sup>2-</sup>/*t<sub>c</sub>* (Table 1) are also given in Fig. 9A as a function of *t<sub>c</sub>*. In addition, Fig. 9B shows the normalized reduction peak area for Pt in Pt/ZrOSO<sub>4</sub> after calcination *in situ* at 100, 200, and 300°C.

Relevant XPS data are displayed in Fig. 10. Figure 10c shows the XPS signal of Pt(4f) in a sample prepared by impregnating Zr(OH)<sub>4</sub> with PtCl<sub>4</sub> (4 wt% Pt) followed by drying at room temperature. It is seen that the Pt(4f) signal is composed of a single doublet corresponding to a Pt(4f<sub>7/2</sub>) binding energy of 72.9 eV. On the contrary, when PtCl<sub>4</sub> was supported on zirconium sulfate followed by drying at room temperature, two Pt(4f) doublets were found (Fig. 10a) corresponding to Pt(4f<sub>7/2</sub>) binding energies of 71.4 and 73.2 eV. The relative intensities of these signals were 62 and 38%, respectively. Upon *in situ* calcination of this sample in air at 300°C for 2 h, the Pt(4f<sub>7/2</sub>) high binding energy feature disappeared. Only a single doublet with a Pt(4f<sub>7/2</sub>) binding energy of 71.1 eV remained (Fig. 10b). Similar behavior was observed when H<sub>2</sub>PtCl<sub>6</sub> was used as the starting material instead of PtCl<sub>4</sub>.

## DISCUSSION

Let us first deal with the state of Pt in precalcined Pt/ZrO<sub>2</sub>/SO<sub>4</sub><sup>2-</sup>/*t<sub>c</sub>* samples. Literature data show that the reduction temperature of precalcined supported Pt catalysts depends on a number of parameters, in particular the Pt loading, the nature of the support, and the pretreatment conditions. However, this temperature very seldom exceeds 300°C (12, 13, 17, 18). We therefore concur that the TPR peaks below 200°C in Fig. 1 correspond to the reduction of Pt. Analysis of the gas phase by mass spectrometry showed that these TPR peaks were accompanied only by a decrease in H<sub>2</sub> partial pressure. Moreover, for *t<sub>c</sub>* < 400°C, the amount of consumed hydrogen corresponded to a H/Pt ratio of about 3.95, indicating a complete reduction of Pt. As seen in Fig. 1, the reduction temperature decreased almost linearly as a function of calcination temperature up to *t<sub>c</sub>* = 550°C, indicating that as *t<sub>c</sub>* increases, the interactions between PtO<sub>2</sub> and ZrO<sub>2</sub> decrease. As reported by other workers (13, 19) we found that unsupported PtO<sub>2</sub> (i.e., no interaction with support) reduces swiftly below room temperature. In our case, it is believed that as *t<sub>c</sub>* increases, the size of PtO<sub>2</sub> particles

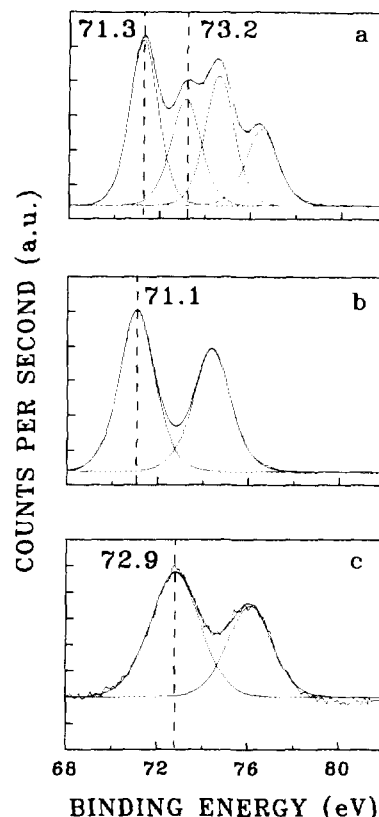


FIG. 10. Pt(4f) XPS spectra of (a) PtCl<sub>4</sub>/ZrOSO<sub>4</sub> dried at room temperature, (b) PtCl<sub>4</sub>/ZrOSO<sub>4</sub> calcined *in situ* at 300°C, and (c) PtCl<sub>4</sub>/Zr(OH)<sub>4</sub> dried at room temperature.

also increases and their interactions with the support become weaker; therefore their reduction temperature decreases. Note that at low calcination temperature, i.e.,  $t_c \leq 300^\circ\text{C}$ , Pt may still be in the form of a complex involving O and Cl (20) and not as  $\text{PtO}_2$ . It is worthy to note also that as far as the relationship between the Pt reduction temperature and  $t_c$  is concerned, the opposite trend seems to occur for  $\text{Al}_2\text{O}_3$ -supported Pt catalysts (17).

As  $t_c$  exceeds  $300^\circ\text{C}$ , the Pt reduction peak decreases and eventually vanishes at  $t_c = 600^\circ\text{C}$  (Table 1). Since our temperature ramp during TPR begins at room temperature, we cannot detect any reduction that takes place at subambient temperatures. However, the absence of Pt reduction peaks during TPR of  $\text{Pt}/\text{ZrO}_2/\text{SO}_4^-/t_c$  with  $t_c \geq 600^\circ\text{C}$  cannot be explained on this basis. Indeed, exposure of  $\text{Pt}/\text{ZrO}_2/\text{SO}_4^-/600$  to pulses of 10%  $\text{H}_2/\text{Ar}$  at room temperature gave a H/Pt ratio of only 0.05. An alternative explanation is that under air calcination at temperatures above  $600^\circ\text{C}$ , Pt undergoes reduction to the metallic state. The lack of  $\text{H}_2$  chemisorption at room temperature would then be related to sulfur poisoning (11). Earlier XPS data support this interpretation (16). Moreover, Fig. 7c shows that  $\text{Pt}/\text{ZrO}_2/\text{SO}_4^-/600$  exhibits XRD peaks characteristic of metallic platinum.

A TPR profile similar to those reported here for  $\text{Pt}/\text{ZrO}_2/\text{SO}_4^-/t_c$  samples with  $t_c \geq 600^\circ\text{C}$  has been reported recently by Hattori and co-workers (21–23), with their TPR peak temperature ( $530^\circ\text{C}$ ) being slightly higher than what we observed ( $450^\circ\text{C}$ ). The authors attributed this peak to the reduction of both Pt and sulfate ions, and concluded as in their earlier work (9) that Pt on sulfated zirconia is extremely difficult to reduce. This conclusion appears to be untenable.

As to how the Pt reduction takes place under air treatment, two suggestions may be made: (i) thermal decomposition of Pt oxide; (ii) reduction of Pt oxide by sulfur-containing species. Both processes have been reported in the literature. Escard *et al.* (24) reported that under flowing  $\text{O}_2$  or inert gas, unsupported  $\text{H}_2\text{PtCl}_6$  decomposes stepwise to metallic platinum at  $520^\circ\text{C}$ . There are also indications that supported  $\text{PtO}_2$  decomposes in  $\text{O}_2$  above  $600^\circ\text{C}$  to give metallic platinum (13). On the other hand, Löff *et al.* (25) found that oxidized Pt can be reduced to the metallic state at  $500^\circ\text{C}$  in the presence of gaseous  $\text{SO}_2$  even along with oxygen.

Based only on Figs. 1 and 6, and ignoring the effect of reoxidation, the following proposal may be made. Figures 1 and 6 show that using sulfated and nonsulfated samples with the same Pt content, and precalcined under identical conditions, formation of metallic Pt in  $\text{Pt}/\text{ZrO}_2/t_c$  starts slowly at  $t_c = 650^\circ\text{C}$  and is complete only at  $800^\circ\text{C}$  (Figs. 6 and 7); on the other hand, for  $\text{Pt}/\text{ZrO}_2/\text{SO}_4^-/t_c$  samples, the formation of metallic platinum is complete at a calcination temperature of  $600^\circ\text{C}$  (Figs. 1 and 7). Therefore, it

may be concluded that since  $\text{Pt}/\text{ZrO}_2/\text{SO}_4^-/t_c$  reduces in air at a lower calcination temperature than  $\text{Pt}/\text{ZrO}_2/t_c$ , the mechanism involved must be different and may involve sulfur species.

However, these observations may be erroneous because the samples used in Figs. 1 and 6 had been precalcined and stored in ambient air. Metallic Pt may have formed during calcination and reoxidized during storage. Since it is known that reoxidation of metallic Pt is strongly dependent on particle size (26), an alternative proposal should also be considered. It may be argued that in the absence of sulfur species, small oxide particles are formed. The decomposition of this oxide leads to small metallic Pt particles which will be readily reoxidized under ambient conditions. On the contrary, in the presence of sulfur, platinum oxide and consequently Pt metallic particles are larger and the reoxidation is more difficult. Therefore, the following question must be addressed: How do we discriminate between the actual effect of calcination on the state of Pt and any further reoxidation that may take place during storage?

Comparison between Figs. 9A and 9B provides an appropriate answer to this question. Figure 9A shows the combined effect of calcination and reoxidation in ambient air on the state of Pt, whereas Fig. 9B shows only the effect of *in situ* calcination. It is seen that even in the absence of sulfur species, Pt undergoes significant reduction during calcination at temperatures as low as  $300^\circ\text{C}$  (Fig. 9Ba). However, in all cases, at the same calcination temperature, the extent of Pt reduction is higher in  $\text{Pt}/\text{ZrO}_2/\text{SO}_4^-$  than in  $\text{Pt}/\text{ZrO}_2$ . This may be due to a *direct* and/or an *indirect* effect of sulfur species. The presence of sulfur may weaken the interaction between the support and the platinum oxide particles, thus allowing them to grow larger than in the absence of sulfur. This makes it easier for  $\text{PtO}_2$  to decompose giving rise to large metallic Pt difficult to reoxidize. This is what is referred to as *indirect* effect. By *direct* effect we mean the actual involvement of sulfur species in the reduction process of Pt.

Data shown in Table 1 provide evidence for the *indirect* effect of sulfur. It is seen that at the same calcination temperature, hydrogen reduction of Pt on pure zirconia is more difficult than the reduction of Pt on sulfated zirconia, for it takes place at a higher temperature. This indicates that the presence of sulfate ions weakens the interaction between Pt-containing species and the support, and may explain the lower dispersion of Pt in sulfated samples (23). As for nonsulfated  $\text{Pt}/\text{ZrO}_2$ , comparison between Figs. 9Aa and 9Ba leads to the following conclusions:

(i) Calcination at  $t_c \leq 200^\circ\text{C}$  had no effect on the oxidation state of Pt, probably because Pt(IV) was still stabilized in a complex containing O and Cl (20).

(ii) At  $t_c$  in the range  $300$ – $600^\circ\text{C}$ , about 75% of the

platinum reduces by thermal decomposition during air precalcination. The metallic Pt particles formed under calcination conditions are most probably quite small as they fully reoxidize during storage (Fig. 9Aa) and the oxide thus formed reduces under hydrogen at a constant temperature, i.e., 175–180°C (Table 1). It is suggested that the remaining 25% PtO<sub>2</sub> is in strong interaction with the support and does not decompose in air at 300–600°C.

(iii) As  $t_c$  increases above 600°C, more and more PtO<sub>2</sub> is decomposed and the metallic particles obtained are larger and more resistant to reoxidation in ambient air. Eventually at  $t_c = 800^\circ\text{C}$ , all PtO<sub>2</sub> decomposes to large metallic particles that do not reoxidize during storage (Figs. 6 and 7).

The effect of the calcination temperature on the state of Pt in sulfated Pt/ZrO<sub>2</sub>/SO<sub>4</sub><sup>-</sup> samples follows a similar pattern. However, some significant differences may be pointed out:

(i) Even at  $t_c = 200^\circ\text{C}$  about 50% of Pt was reduced during calcination (Fig. 9Bb). This may indicate a direct involvement of sulfur species in the reduction process.

(ii) At  $t_c$  in the range 300–500°C, about 20% of the platinum resisted reduction during calcination (Fig. 9Bb). However, some of the reduced Pt particles were large enough to resist reoxidation during storage (Fig. 9Ab). This may indicate that PtO<sub>2</sub> particles grow larger in the presence of sulfur species and give rise to large metallic particles and/or the presence of sulfur facilitates the sintering of metallic Pt.

(iii) At  $t_c = 600^\circ\text{C}$ , all Pt is reduced in large metallic particles that do not reoxidize in ambient air (Figs. 1 and 7). Scanning electron microscopy showed that in Pt/ZrO<sub>2</sub>/SO<sub>4</sub><sup>-</sup>/600 (5 wt% Pt), the size of some particles is as high as 300 nm (7).

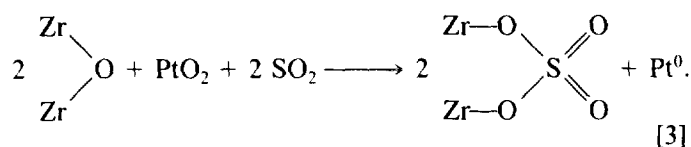
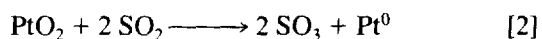
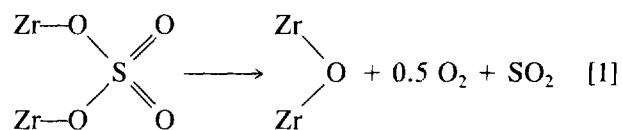
In summary, the presence of sulfur species weakens the interactions between the PtO<sub>2</sub> particles and the support. This allows the Pt oxide particles to grow larger than in nonsulfated samples, and to give by decomposition large metallic Pt particles difficult to reoxidize in ambient air (or during cooling).

In addition to this indirect effect of sulfur species on the state of Pt, there are several indications of a *direct* involvement of sulfur species in the reduction process of Pt during calcination. This effect is inferred by the dependence of the calcination temperature at which the reduction occurs upon the relative contents of Pt and sulfur. Indeed, this temperature can be lowered significantly by increasing the sulfur content. The most straightforward way to address this issue is to use zirconium sulfate as support. Figure 9Bc shows that after *in situ* treatment in dry air at a temperature as low as 100°C, about 50% of the Pt in Pt/ZrOSO<sub>4</sub> was reduced. At 200°C, the reduction of Pt was almost complete.

XPS data (Fig. 10) show even more dramatic effects of

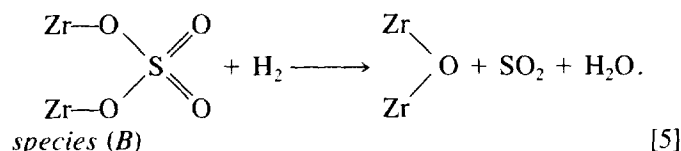
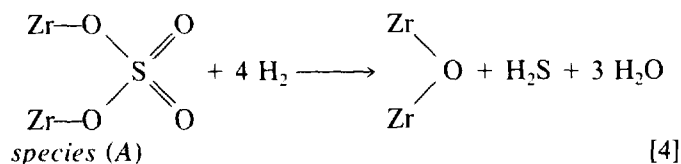
sulfur. Assignment of the Pt(4f) XPS peaks was made following the same reasoning as in our earlier work (16). Peaks corresponding to a Pt(4f<sub>7/2</sub>) binding energy below 71.6 eV were assigned to metallic Pt, and Pt(4f<sub>7/2</sub>) peaks corresponding to higher binding energies were attributed to oxidized Pt. Figure 10a shows that in PtCl<sub>4</sub> supported on zirconium sulfate (ZrOSO<sub>4</sub>), platinum was partly reduced even at room temperature. In terms of surface composition, 62% of the Pt was reduced. This could be compared to the 50% bulk reduction obtained after *in situ* treatment in dry air at 100°C (Fig. 9Bc). Upon *in situ* calcination of PtCl<sub>4</sub>/ZrOSO<sub>4</sub> in flowing air at 300°C, Pt fully reduces to the metallic state (Fig. 10b). The partial reduction of Pt on ZrOSO<sub>4</sub> at room temperature cannot be attributed to the effect of high vacuum or X-rays in the XPS chamber. Indeed, as shown in Fig. 10c, Pt remains fully oxidized when supported on Zr(OH)<sub>4</sub> instead of ZrOSO<sub>4</sub> and dried at room temperature.

There is indication in the literature (25) that oxidized Pt can be reduced to the metallic state at 500°C in the presence of gaseous SO<sub>2</sub> even along with oxygen. It is believed that a similar mechanism operates in our case, the SO<sub>2</sub> originating from the decomposition of sulfate ions as shown by mass spectrometry in this work and others (27). The overall equations of SO<sub>2</sub> formation (Eq. [1]) and PtO<sub>2</sub> reduction (Eqs. [2] and [3]) may be tentatively represented as follows:



As for the sulfur-containing species, Figs. 1 and 4 clearly indicate the presence of at least two different sulfate species. During TPR of Pt/ZrO<sub>2</sub>/SO<sub>4</sub><sup>-</sup>/ $t_c$  with  $t_c < 600^\circ\text{C}$ , one of these species generates H<sub>2</sub>S while the other gives rise to SO<sub>2</sub>. For Pt-free samples, both sulfate species generate SO<sub>2</sub>. These species are designated hereafter as (A) and (B), respectively. Only species (A) was left in samples calcined at  $t_c \geq 600^\circ\text{C}$  regardless of whether Pt was present or not. Comparison of Figs. 1 and 4 shows that in the presence of Pt both sulfate species reduce at lower temperatures. This is most probably related to the availability of atomic hydrogen *via* hydrogen spillover

(11, 14). It is proposed that the sulfate reduction takes place according to the following equations:



It is difficult to identify the exact nature of these sulfate species. A number of infrared studies of sulfated oxides indicated the presence of more than one sulfur containing species (28–30). Bensitel *et al.* (29) found that all species are of the  $(\text{MO})_3\text{S}=\text{O}$  type, i.e., they do not have coupled  $\text{S}=\text{O}$  oscillators. Most other authors proposed the presence of bidentate sulfate. Nonetheless, these species remain ill-defined.

In our case, we observed that during TPR of a 4 wt% Pt on zirconium sulfate samples calcined at 300 or 600°C, most of the sulfate reduces to  $\text{SO}_2$  and not to  $\text{H}_2\text{S}$  as in  $\text{Pt}/\text{ZrO}_2/\text{SO}_4^-/t_c$  (compare Figs. 2 and 8). Moreover, in this sample the relative content of species (A) increases as the calcination temperature increases. We therefore tentatively assign species (A) to the bidentate sulfate species identified by a number of authors (28, 31). The sharpness of the reduction peak of species (B) in  $\text{Pt}/\text{ZrO}_2/\text{SO}_4^-/t_c$  ( $t_c < 600^\circ\text{C}$ ) as shown in Fig. 1 indicates that this is a well-defined species. Moreover, since this species is very abundant in  $\text{Pt}/\text{ZrOSO}_4$ , it is proposed that (B) is a structural sulfate species rather than an adsorbed one. Work is in progress to unravel this problem.

### CONCLUSION

The following conclusions may be drawn:

(i) The effect of sulfur species on the state of Pt during air calcination of Pt on sulfated zirconia superacid catalysts is twofold. They have an *indirect* effect leading to a weaker interaction between Pt oxide and the support. This in turn allows the oxide particles to grow larger than in the absence of sulfur. These large particles are easier to decompose and give large metallic particles hard to reoxidize. In addition, sulfur species have a *direct* effect on the state of Pt during calcination for they are involved in the reduction processes. The reducing agent is believed to be  $\text{SO}_2$  produced by the decomposition of sulfate species.

(ii) TPR profiles indicate the presence of two different

sulfate species. These species were tentatively assigned to adsorbed and structural sulfate.

### ACKNOWLEDGMENTS

This work is supported by Strategic Grant (STR0117964) from the Natural Sciences and Engineering Research Council of Canada (NSERC) and partly by EMR Canada and by Imperial Oil, Ltd. A.D. is grateful to the Ivory Coast Government for a scholarship. We thank Dr. B. Grandjean for the use of the mass spectrometer, and also Drs. I. Wender, B. Davis, and S. C. C. Chuang for helpful discussions.

### REFERENCES

1. Yamaguchi, T., *Appl. Catal.* **61**, 1 (1990).
2. Arata, K., *Adv. Catal.* **37**, 165 (1990).
3. Yamaguchi, T., Tanabe, K., and Kung, Y. C., *Mater. Chem. Phys.* **16**, 27 (1986).
4. Tanabe, K., and Yamaguchi, T., *Stud. Surf. Sci. Catal.* **44**, 99 (1989).
5. Wen, M. Y., Wender, I., and Tierney, J. W., *Energy Fuels* **4**, 372 (1990).
6. Hosoi, T., Shimadzu, T., Itoh, S., Baba, S., Takaoka, H., Imai, T., and Yokoyama, N., *Prepr.—Am. Chem. Soc., Div. Pet. Chem.* **33**, 562 (1988).
7. Dicko, A., M. Sc. Thesis, Laval University, (1994).
8. Ebitani, K., Konishi, J., and Hattori, H., *J. Catal.* **130**, 257 (1991).
9. Ebitani, K., Konno, H., Tanaka, T., and Hattori, H., *J. Catal.* **135**, 60 (1992).
10. Ebitani, K., Konishi, J., Horie, A., Hattori, H., and Tanabe, K., in "Acid-Base Catalysis" (K. Tanabe, H. Hattori, T. Yamaguchi, and T. Tanaka, Eds.), p. 491. VCH Verlag, Weinheim, 1989.
11. Iglesia, E., Soled, S. L., and Kramer, G. M., *J. Catal.* **144**, 238 (1993).
12. Ebitani, K., and Hattori, H., *Bull. Chem. Soc. Jpn.* **64**, 242 (1991).
13. Yao, H. C., Sieg, M., and Plummer, H. K., Jr., *J. Catal.* **59**, 365 (1979).
14. Ebitani, K., Tsuji, J., Hattori, H., and Kita, H., *J. Catal.* **135**, 609 (1992).
15. Paál, Z., Muhler, M., and Schlögl, R., *J. Catal.* **143**, 318 (1993).
16. Sayari, A., and Dicko, A., *J. Catal.* **145**, 561 (1994).
17. Isaacs, B. H., and Petersen, E. E., *J. Catal.* **77**, 43 (1982).
18. Sexton, B. A., Hughes, A. E., and Fogar, K., *J. Catal.* **77**, 85 (1982).
19. Park, S. H., Tzou, M. S., and Sachtler, W. M. H., *Appl. Catal.* **35**, 85 (1986).
20. Burch, R., *J. Catal.* **71**, 348 (1981).
21. Ebitani, K., Konno, H., Tanaka, T., and Hattori, H., *J. Catal.* **143**, 322 (1993).
22. Hattori, H., *Stud. Surf. Sci. Catal.* **77**, 69 (1993).
23. Ebitani, K., Tanaka, T., and Hattori, H., *Appl. Catal. A: General*, **102**, 79 (1993).
24. Escard, J., Pontvianne, B., Chenebaux, M. T., and Cosyns, J., *Bull. Soc. Chim. Fr.* 2399 (1975).
25. Lööf, P., Kasemo, B., Björnkvist, L., Andersson, S., and Frestad, A., *Stud. Surf. Sci. Catal.* **71**, 253 (1991).
26. Chmelka, B. F., Went, G. T., Csencsits, R., Bell, A. T., Petersen, E. E., and Radke, C. J., *J. Catal.* **144**, 506 (1993).
27. Lee, J. S., and Park, D. S., *J. Catal.* **120**, 46 (1989).
28. Yamaguchi, T., Jin, T., and Tanabe, K., *J. Phys. Chem.* **90**, 3148 (1986).
29. Bensitel, M., Saur, O., Lavalley, J. C., and Morrow, B. A., *Mater. Chem. Phys.* **19**, 147 (1988).
30. Morterra, C., Cerrato, G., Emanuel, C., and Bolis, V., *J. Catal.* **142**, 349 (1993).
31. Sohn, J. R., and Kim, H. W., *J. Mol. Catal.* **52**, 361 (1989).